

Giant electroviscous effects in a ferroelectric nematic liquid crystal

M. Praveen Kumar¹, Jakub Karcz², Przemyslaw Kula², Smarajit Karmakar³ and Surajit Dhara^{1*}

¹*School of Physics, University of Hyderabad, Hyderabad-500046, India*

²*Institute of Chemistry, Faculty of Advanced Technologies and Chemistry, Military University of Technology, Warsaw, Poland.*

³*Tata Institute of Fundamental Research, Hyderabad, 500107, India*

(Dated: March 21, 2023)

The electroviscous effect deals with the change in the viscosity of fluids due to an external electric field. Here, we report experimental studies on the electroviscous effects in a ferroelectric nematic liquid crystal. It was synthesised accomplishing a new synthetic route which provides higher yield than conventional one. We measure electric field-dependent viscosity under a steady shear at different temperatures. In the low field range, the increase in viscosity ($\Delta\eta = \eta(E) - \eta_0$) is proportional to E^2 and the corresponding viscoelectric coefficient ($f \approx 10^{-9} \text{ m}^2/\text{V}^2$) of the ferroelectric nematic is 2 orders of magnitude larger than the apolar nematic liquid crystals and largest ever measured for a fluid. The apparent viscosity measured under a high electric field shows a power-law divergence $\eta \sim (T - T_c)^{-0.7 \pm 0.05}$, followed by nearly an order of magnitude drop below the N-N_F phase transition. Experimental results within the dynamical scaling approximation demonstrate rapid growth of polar domains under a strong electric field as the N-N_F phase transition is approached. The gigantic electroviscous effects demonstrated here are important for emerging applications and understanding striking electrohydromechanical effects in ferroelectric nematic liquid crystals.

Nematic (N) liquid crystals (LCs) are widely used in flat panel displays. They are apolar i.e., the mean molecular direction, called the director \hat{n} is equivalent to $-\hat{n}$, hence there is no macroscopic polarisation [1]. Long ago Max Born predicted the existence of polar nematic i.e., the ferroelectric nematic [2]. However, such a phase was elusive for a long time. Very recently the ferroelectric nematic phase (N_F) has been discovered in a highly polar with slightly wedge-shaped molecules [3–9]. It has created a lot of interest in the science and engineering community because of its technological applications and intriguing phenomena important for fundamental science [10–16]. The ferroelectric nematic has high potential to replace the existing non-polar nematics in displays because of its striking electro-optical properties and fast response time [9, 17, 18]. Although, several new physical and electrooptical properties of N_F phase have been reported [19, 21–26, 52] their flow viscosities and the effect of external electric field on the flows are yet unexplored. Since the constituent molecules are highly polar the electroviscous effects in ferroelectric NLCs are expected to be more robust than in ordinary nematic liquid crystals due to the interaction of polarisation with the electric field.

The electroviscous effect deals with the change in viscosity especially in polar liquids in the presence of the electric field. The electric field-dependent viscosity of such liquids can be expressed as [27, 28]

$$\eta(E) = \eta_0(1 + f|E|^2) \quad (1)$$

where η_0 is the viscosity in the absence of the field and f is the viscoelectric coefficient. For many organic liquids including water, $f \sim 10^{-13} - 10^{-16} \text{ m}^2\text{V}^{-2}$ [27, 29]. When the fluid is a nematic liquid crystal (NLC) the viscosity depends on the orientation of the director with

respect to the flow direction. There are three flow viscosity coefficients of nematics which are known as Miesowicz viscosities [30, 31]. In the case of η_1 , the director is perpendicular to the flow direction i.e., $\hat{n} \perp \vec{v}$ and parallel to the velocity gradient i.e., $\hat{n} \parallel \vec{\nabla}v$. For η_2 , the director is parallel to the flow direction i.e., $\hat{n} \parallel \vec{v}$. In the case of η_3 the director is perpendicular to both the velocity and velocity gradient directions, i.e., $\hat{n} \perp \vec{v}$ and $\hat{n} \perp \vec{\nabla}v$. Usually for calamitic liquid crystals (rod-like molecules) $\eta_1 > \eta_3 > \eta_2$ [1, 32–34]. These viscosity coefficients depend on the molecular structure as well as on the intermolecular interactions and usually increase with decreasing temperature [35, 36].

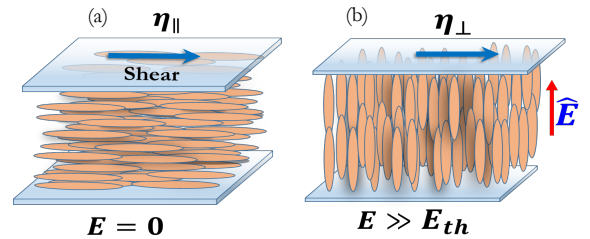


FIG. 1. Orientation of the LC director \hat{n} without and with electric field, E . (a) In the absence of an electric field, \hat{n} is parallel to the flow direction (blue arrow) and the apparent viscosity $\eta \simeq \eta_{||}$. (b) Above the Fredericksz threshold field $E \gg E_{th}$, \hat{n} is perpendicular to the flow direction and the apparent viscosity $\eta \simeq \eta_{\perp}$.

There are a few studies on the effect of electric field on the flow viscosities of ordinary NLCs [35–41]. In the absence of an electric field, the director \hat{n} of the presheared nematic is parallel to the shear-flow direction and we can write the apparent viscosity $\eta \simeq \eta_2 \simeq \eta_{||}$ (Fig.1(a)).

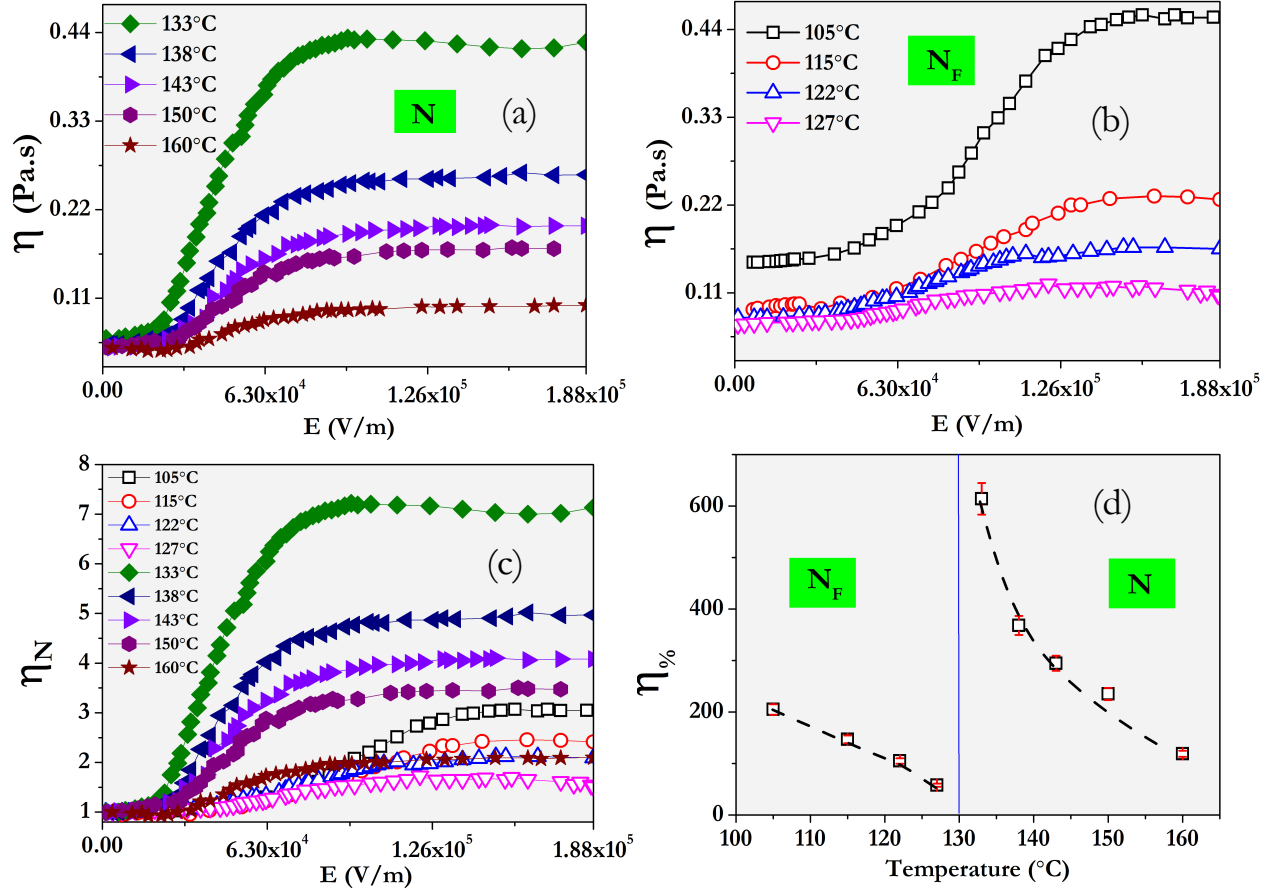


FIG. 2. Change of apparent viscosity η with field at different temperatures in the (a) N and (b) N_F phases. Measurements are made at a shear rate $\dot{\gamma} = 120 \text{ s}^{-1}$. (c) Normalized viscosity, $\eta_N = \frac{\eta(E)}{\eta_0}$ in both phases, where η_0 is the constant viscosity in the absence of the electric field. (d) The percentage increment of viscosity, $\eta_{\%} = \frac{\eta(E=E_s) - \eta_0}{\eta_0} \times 100$, at different temperatures, where E_s is the field above which the viscosity is saturated. We chose $1.7 \times 10^5 \text{ V/m}$. The vertical line indicates N- N_F phase transition temperature. Dashed line is a guide to the eye.

Preshear is necessary to get a uniform alignment of the liquid crystal director. For a NLC with positive dielectric anisotropy, above the Fredericksz threshold electric field (E_{th}), \hat{n} reorients toward the field direction and the apparent viscosity increases and saturates at higher fields and $\eta \simeq \eta_{\parallel} \simeq \eta_{\perp}$ (Fig.1(b)). Here, η_{\parallel} and η_{\perp} are the viscosities of the NLCs with the director \hat{n} parallel and perpendicular to the flow direction, respectively. The rising part of the viscosity from zero fields to the onset of saturation can be expressed by Eq.(1) and the coefficient f can be regarded as the viscoelectric coefficient of the nematic liquid crystal. It signifies the growth rate of the electroviscosity due to the applied electric field.

RESULTS AND DISCUSSION

We work with a ferroelectric nematic liquid crystal RM-734, first reported by Mandle *et al.* [3]. We have developed a new method for diester liquid crystal syn-

thesis. It is based on the inversion of molecular core expansion (see Materials section). With such an approach, the overall yield of the synthesis is increased and the possibility of obtaining highly fluorinated liquid crystal diesters, especially those bearing fluorine atoms in the central phenyl ring is enhanced. The description of our novel approach and the synthesis summary are presented in the supplementary [42]. We set up a computer-controlled electrorheological experiment based on a rheometer. The measuring device consists of two parallel plates with a fixed gap connected to an LCR meter and interfaced with a computer. The setup is capable of measuring the viscosity and the dielectric constant simultaneously (supplementary information [42]). First, we measured electric field-dependent viscosity, known as apparent viscosity at different temperatures by changing the amplitude of the electric field at a fixed frequency. The viscosity of the presheared sample is independent of the shear rate (SI) [42], hence we fixed the shear rate $\dot{\gamma} = 120 \text{ s}^{-1}$ for all measurements. Figure 2(a) shows the variation of appar-

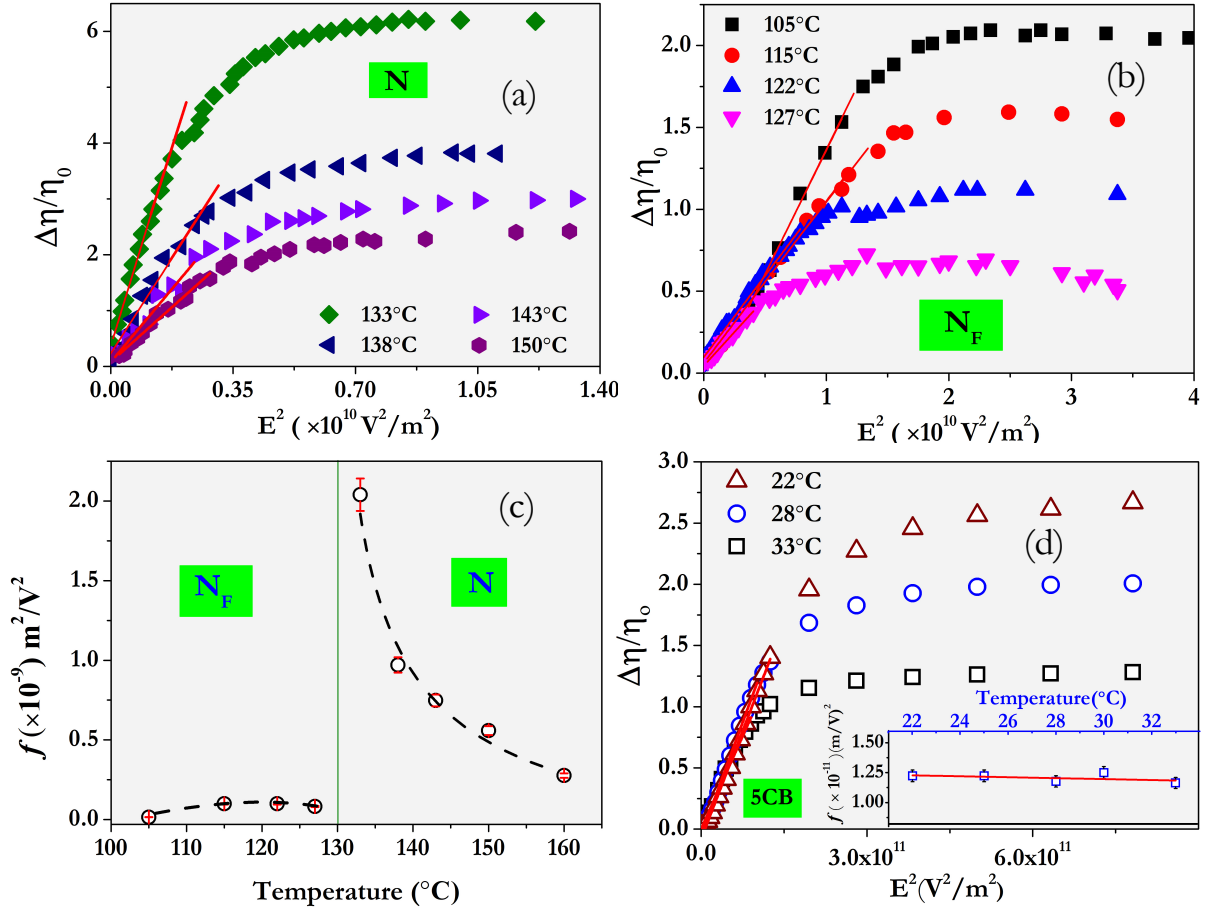


FIG. 3. Variation of $\Delta\eta/\eta_0$ with E^2 at different temperatures in (a) N and (b) N_F phases. The red lines are best fit to the linear part of the curves. (c) Variation of viscoelectric coefficient f with temperature. Dashed line is a guide to the eye. The vertical line indicates N- N_F phase transition temperature. (d) Variation of $\Delta\eta/\eta_0$ with E^2 of 5CB at a few temperatures. Shear rate $\dot{\gamma} = 120 \text{ s}^{-1}$. Inset shows variation of f with temperature of 5CB LC.

ent viscosity η at different temperatures in the nematic (N) phase of RM-734. The viscosity below a particular field (Freedericksz threshold, $E_{th} \simeq 2.5 \times 10^4 \text{ V/m}$) is constant ($= \eta_0$) and it rises rapidly with the field and saturates above $E \simeq 1.0 \times 10^5 \text{ V/m}$. Figure 2(b) shows the variation of apparent viscosity at different temperatures in the N_F phase. In this phase, the viscosity shows similar trends but the relative enhancement of viscosity with respect to the zero field viscosity is smaller compared to that of the N phase. In order to bring out the difference we introduce normalised viscosity, defined as $\eta_N = \frac{\eta(E)}{\eta_0}$, where η_0 is the zero-field viscosity (Fig.2(c)). It is noted that the change of saturated viscosity with temperature is non-monotonic. For example, the saturated viscosity increases as the temperature is raised from 160°C and reach a maximum value at the N- N_F transition and then decreases drastically as the temperature is reduced. Figure 2(d) shows the relative enhancement of viscosity in terms of percentage, which can be written as $\eta\% = \frac{\eta(E=E_s) - \eta_0}{\eta_0} \times 100$, where $\eta(E = E_s)$ is the

saturated viscosity. The percentage increment of viscosity $\eta\%$ increases rapidly as the N- N_F phase transition is approached and the pronounced effect is observed very close to the N- N_F transition temperature where the enhancement is about 600%. Below the phase transition, it drastically decreases to 50% ($T = 127^\circ\text{C}$) and again gradually increases to 200% which will be discussed later.

We have obtained the viscoelectric coefficient f at different temperatures using Eq.(1) which can be expressed as $\Delta\eta/\eta_0 = fE^2$, where $\Delta\eta = \eta(E) - \eta_0$. Figure 3(a) and (b) shows the variation of $\Delta\eta/\eta_0$ with E^2 in N and N_F phases, respectively. The coefficient f is obtained from the slope of the linear part of the curve in the low field region (below the onset of saturation) and shown in Fig. 3 (c). In the N phase (e.g., $T=160^\circ\text{C}$) $f = 0.4 \times 10^{-9} \text{ m}^2\text{V}^{-2}$ and it increases rapidly as the N- N_F transition is approached. The maximum value is obtained ($f = 2.1 \times 10^{-9} \text{ m}^2\text{V}^{-2}$) near N- N_F transition temperature. This is about six orders of magnitude larger than that of ordinary liquids like water [27, 29] and the

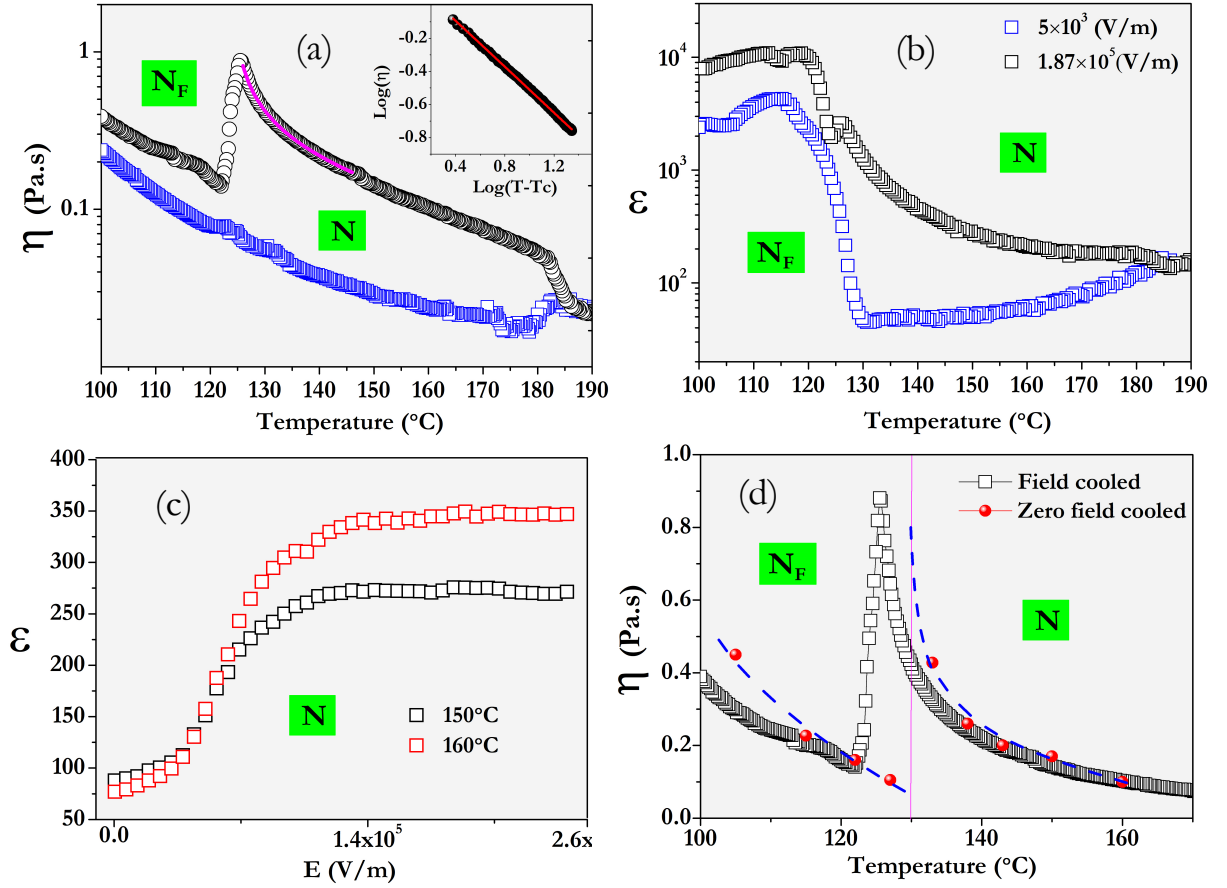


FIG. 4. (a) Temperature dependence of apparent viscosity η measured at $\dot{\gamma} = 120 \text{ s}^{-1}$, at two electric fields. Blue squares correspond to data measured at $E = 5 \times 10^3 \text{ V/m}$ ($\ll E_{th}$) and black circles correspond to data measured at $E = 1.87 \times 10^5 \text{ V/m}$ ($\gg E_{th}$). Inset shows a power-law fit to $\eta \sim (T - T_c)^{-0.7 \pm 0.05}$ to the diverging viscosity where $T_c = 124.13^\circ\text{C}$. Magenta curve indicates the temperature range selected for fitting. (b) Temperature dependence of effective dielectric constant ϵ measured at $f = 600 \text{ Hz}$. (c) Variation of ϵ with field at two temperatures in the N phase. (d) Growth of viscosity η as a function of temperature in two different conditions. One with the electric field E on. This is referred to here as “field-cooled” (black squares, $E = 1.87 \times 10^5 \text{ V/m}$) and the other set (red dots) are obtained from Fig. 2(a,b) where the system is cooled to the lower temperature first and then the field is applied to measure the viscosity. Dashed blue line is a guide to the eye for zero-field cooled data. The vertical line indicates N-N_F transition temperature under zero-field.

largest ever measured for a fluid.

In order to compare the same with ordinary NLCs with polar molecules we measured the viscoelectric coefficient of 5CB (pentyl cyanobiphenyl) liquid crystal. Figure 3(d) shows a change in apparent viscosity with the electric field at a few temperatures and corresponding f of 5CB LC. The coefficient f ($\simeq 1.25 \times 10^{-11} \text{ m}^2\text{V}^{-2}$) is independent of temperature and almost two orders of magnitude smaller than RM-734 liquid crystal. The molecules of 5CB have an axial dipole moment of 4.8 D [43] which is almost two and a half times smaller than compound RM-734 (11.3 D) [6]. Thus, due to the large dipole moment and resulting dipole-dipole correlation, the viscoelectric coefficient of RM-734 is expected to be much higher than nematics with nonpolar or weakly polar molecules. However, two orders of magnitude larger f of RM-734 and its rapid growth indicate the emergence of polar domains

that grows rapidly as the N-N_F transition is approached.

In what follows, we have measured the temperature-dependent apparent viscosity η of a presheared sample. We fixed the shear rate $\dot{\gamma} = 120 \text{ s}^{-1}$, and measured the viscosity $\eta_{||}$ ($E \ll E_{th}$) and η_{\perp} ($E \gg E_{th}$) as a function of temperature (Fig. 4(a)). The viscosity increases with decreasing temperature as expected. No significant change in $\eta_{||}$ is observed at the N-N_F transition temperature ($T = 130^\circ\text{C}$). On the other hand η_{\perp} increases much more rapidly with decreasing temperature and tends to diverge at the N-N_F transition temperature. It reaches a maximum of 900 mPas at the transition and the corresponding viscosity anisotropy $\delta\eta = \eta_{\perp} - \eta_{||} = 750 \text{ mPas}$, which is nearly an order of magnitude larger than the ordinary NLCs [32, 35, 38] and largest viscosity anisotropy ever measured for any NLC. It is noted that η_{\perp} changes slope below temperature $T = 150^\circ\text{C}$, at which the collec-

tive behaviour of the molecules starts to develop [7]. Below the N-N_F transition the viscosity drops down significantly to about 140 mPas from 900 mPas, showing η_{\perp} of the N_F phase is reduced compared to the N phase although the orientational order parameter of the N_F phase is larger [4]. Such a drastic decrease of η_{\perp} is consistent with the first-order nature of the N-N_F phase transition and it suggests that microscopically the structure of these two phases are different. Although the dielectric properties of this LC are quite complex [44–46] we could simultaneously measure an effective dielectric constant ϵ (Fig.4(b)) at a frequency of 600 Hz [47]. Since the dielectric anisotropy is positive, $\epsilon \simeq \epsilon_{\perp}$ when $E \ll E_{th}$ and $\epsilon \simeq \epsilon_{\parallel}$ when $E \gg E_{th}$ (Fig.4(c)). It is noted that ϵ_{\parallel} shows a nearly diverging trend followed by a small kink at the N-N_F phase transition temperature (Fig.4(a)). The diverging trend in ϵ_{\parallel} is a signature of cooperative molecular motion possibly leading to polar domains which are basically dynamic clusters of parallel dipoles.

At high temperatures, due to thermal fluctuations, the size of the polar domains should be small, but as the temperature is decreased towards N-N_F transition, the domain size will grow. Higher electric field can enhance parallel correlation of dipoles and facilitate domain growth. Under these conditions, the viscosity is expected to increase, as seen in Fig.4(a) because larger stress will be needed to deform the polar domains. Thus, one does not expect a strong deviation between the measurements of viscosity done in the following two scenarios; (1) with the high field on at high temperature and then cooled to the lower temperature (referred to here as field cooled) and (2) first cooled at the required temperature and then apply the desired electric field (zero field-cooled) and measure the viscosity. In both these scenarios, the domain will grow when the electric field is applied in the N phase, so one expects the measurements to be very similar qualitatively and quantitatively. As shown in Fig.4(d), the data indeed suggest the same (see data for $T > T_c$). The results will be very different below the transition temperature simply because at zero field cooling conditions; the system will go through a sharp structural change due to N to N_F phase transition. On the other hand, in the field-cooled conditions, the polar domains in the N phase will not allow the system to immediately go to the N_F phase and the sharp phase transition will be rounded as evident from Fig.4(d). Although the scenario proposed seems to be quite likely the reason for the observation, we do not have direct proof of the growth of the polar domain with the applied field. Future computational studies on these systems can unearth the microscopic mechanisms for these experimental observations.

If we compare the temperature-dependent viscosity (Fig.4(a)) and dielectric constant (Fig.4(b)) measured at the high field and those at the low field then N-N_F transition temperature at high field is found to be decreased by about 3.5°C. This decrease is not due to the sample

degradation under field [50]. It can be rationalized as caused by the structural changes during the N-N_F phase transition following two possible scenarios. Firstly, the high field can suppress the pre-translational splay fluctuations [6, 48] and favours domain growth with the polarity along the field and hence one would expect the N-N_F transition temperature to decrease if it is considered that the ferronematic phase can have domains with splay structure. Note that the largest applied field in this experiment is not sufficient to align all the molecules along the field direction in the N_F, otherwise, there will not be any phase transition. Secondly, the polar regions will grow in size but they can not span the entire sample as the nematic phase does not support the orientation of all the molecules in the same direction due to large dipole moments. With decreasing temperature, these polar regions grow in size and thus we see a power law change in the measured viscosity in the nematic phase in field-cooled condition. As the temperature is lowered below the equilibrium N-N_F transition, thermodynamically the N_F phase with opposite polarity domains will be favoured as observed in the experiment [9], but the already formed polar regions will oppose the formation of this N_F phase until at a lower temperature where the enthalpy will win over and the system will go to the N_F phase. The near equality of the viscosity data measured in the field-cooled and zero-field-cooled scenarios below the N-N_F phase transition indeed supports this argument. Note that in the latter scenario the splay structure is not essential to explain the observed decrease in the transition temperature.

Further, it is expected that there will be a growth of a length scale related to the formation of polar domains in the nematic phase and if we assume that the length scale shows a divergence at the transition temperature, T_c as $\xi \sim |T - T_c|^{-\nu}$ with ν being the correlation length exponent, then one can expect to see a similar power-law divergence of the viscosity within the dynamical scaling approximation [49] as $\eta \sim \xi^z \equiv |T - T_c|^{-\nu z}$ where z is the dynamical scaling exponent. The power-law fit to the viscosity data is shown in the inset of Fig.4 (a), and the fit is very nice to confirm such a possible power-law divergence of viscosity with an exponent $\nu z \sim 0.7$. Currently, we do not have an independent estimate of the exponent ν , so we can not compute the exponent z . On the other hand, the correlation length exponent in critical phenomena within mean field approximation is $\nu = \frac{1}{2}$, so if we assume the same exponent here, then the dynamical exponent $z \sim 1.4$. This suggests that the domains are probably more elongated (one-dimensional) in nature than spherical. Some of these conjectures can be tested via computer simulation studies which are in progress.

We would like to make a comment here. A one-dimensionally modulated splay structure of the ferroelectric nematic phase of compound RM-734 was proposed by

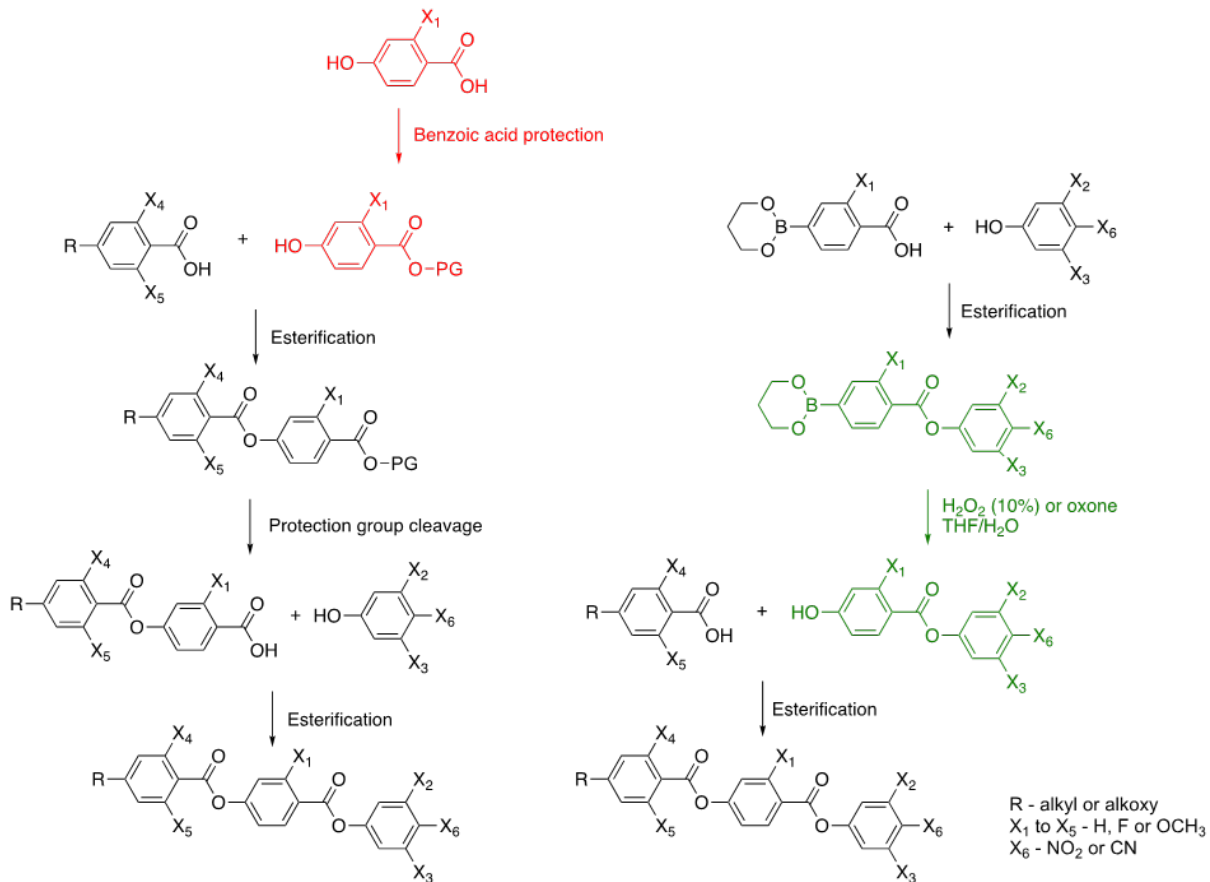


FIG. 5. Comparison of novel synthetic methodology for RM-734 and its fluorinated analogues (right synthetic route) with conventional one (left synthetic route).

Mertelj *et al.* [6] whereas a two-dimensionally modulated splay structure is proposed by the theory [15]. However, Chen *et al.* reported the occurrence of spontaneously polar domains of the opposite sign of polarisation separated by distinct domain boundaries [9]. Our explanation on the temperature-dependent electroviscosity does not rely on any particular structure of the ferroelectric nematic phase.

To summarise, ferroelectric nematic LCs exhibit giant electroviscous effects and the viscoelectric coefficient obtained is the largest ever measured for a fluid. The apparent viscosity under field-cooled condition shows a power-law divergence as the N-N_F transition is approached followed by a drastic decrease below the transition. Large viscoelectric coefficient and pretransitional divergence of the electroviscosity indicate a strong polar correlation resulting in elongated domains that grows rapidly with decreasing temperature. We envisage that the pretransitional growth of polar domains and their dynamic response should be manifested in many other physical properties and effects. The new synthetic route reported here is significant for the large-scale production which is crucial from the application and

broad study perspectives. These new results obtained are important for most of the physical, electrooptical as well as the electrohydromechanical [10–13] effects in ferroelectric nematic liquid crystals. They may also be useful for applications in micro and nanofluidic electromechanical devices (MEMS/NEMS) based on ferroelectric nematic liquid crystals.

MATERIALS

We have developed a new approach for the synthesis of nitro and cyano diesters known for exhibiting ferroelectric character. We have used the opposite direction of molecular core expansion, compared to the known synthetic method [3]. In this method, successive molecular parts are introduced to the molecule concerning the direction of its dipole moment. Four main steps describing this molecular approach are benzoic acid protection, esterification with the appropriate benzoic acid, carboxylic protective group cleavage and, finally, the last esterification reaction. The key half-product

for obtaining the diester derivatives is the eligibly substituted 4-hydroxybenzoic acid. Thus, the protection of carboxylic acid is essential. The benzyl group is used widely for this purpose. This group is not fully selective towards the carboxylic acid, leading to the mixture of protected carboxyl and hydroxyl groups, especially in the case of fluorinated analogues. The yield of the protection of unsubstituted 4-hydroxybenzoic acid is approximately 50% [51]. By introducing the fluorine atom to 4-hydroxybenzoic acid, the yield of the protection reaction significantly decreases [52]. It is because of increasing the acidity of the hydroxyl group caused by the inductive effect. The protection reaction is no longer selective. It limits the use of this method in the case of highly fluorine substituted compounds (Fig.5). In our method, the molecular core expansion direction is inverted. Instead of using a half-product without the regioselectivity towards one of the functional groups, we have used one with a “hidden” precursor of the hydroxyl group. Three main steps characterise our method: esterification of key half-product with an appropriate nitro or cyano phenol, introduction of the hydroxyl group and the final esterification reaction. The key half-product bears a boronic ester group as a “hidden” precursor of the hydroxyl group, which can be performed by the boronic ester oxidation in mild conditions [53]. This reaction, carried out in mild conditions, leads to the corresponding phenol with a high yield. The details of the synthetic scheme of RM-734 is presented in the supplementary [42].

Acknowledgments: SD acknowledges financial support from SERB-SUPRA (Ref. No: SPR/2022/000001). MPK acknowledges UGC-CSIR for fellowship. This work is co-financed by the European Social Fund under the “Operational Programme Knowledge Education Development 2014-2020”. We acknowledge N. V. Madhusudana from Raman Research Institute for the useful discussions. SK acknowledges funding by TIFR (Ref. RTI 4007) and DST (Ref. DST/SJF/PSA-01/2018-19) and SB/SFJ/2019-20/05. PK acknowledges UGB 22-801 project.

* surajit@uohyd.ac.in

- [1] de Gennes, P. G. *The Physics of Liquid Crystals*. Oxford University Press: Oxford, England (1974).
- [2] Born, M. About anisotropic liquids. Attempt at a theory of liquid crystals and the Kerr electric effect in liquids. *Sitzungsber Preuss Akad Wiss.* **30**, 614-650 (1916).
- [3] Mandle, R. J., Cowling, S. J. & Goodby, J. W. Rational Design of Rod-Like Liquid Crystals Exhibiting Two Nematic Phases. *Chem. A Eur. J.* **23**, 14554-14562 (2017).
- [4] Mandle, R. J. & Mertelj, A. Orientational order in the splay nematic ground state. *Phys. Chem. Chem. Phys.* **21**, 18769-18772 (2019).
- [5] Nishikawa, H., Shiroshita, K., Higuchi, H., Okumura, Y., Haseba, Y., Yamamoto, S. I., Koki, S. & Kikuchi, H. A fluid liquid-crystal material with highly polar order. *Adv. Mater.* **29**, 1702354, (2017).
- [6] Mertelj, A., Cmok, L., Sebastián, N., Mandle, R. J., Parker, R. R., Whitwood, A. C., Goodby, J. W., & Čopič, Martin, *Phys. Rev. X* **8**, 041025 (2018).
- [7] Manabe, A., Bremer, M. & Kraska, M. Ferroelectric nematic phase at and below room temperature. *Liq. Cryst.* **48**, 1079-1086 (2021).
- [8] Sebastián, N., Cmok, L., Mandle, R. J., de la Fuente, M. R., Olenik, I. D., Čopič, M. & Mertelj, A., Ferroelectric-ferroelastic phase transition in a nematic liquid crystal *Phys. Rev. Lett.* **124**, 037801 (2020).
- [9] Chen, X., Korblova, E., Dong, D., *et al.* First-principles experimental demonstration of ferroelectricity in a thermotropic nematic liquid crystal: Polar domains and striking electro-optics. *Proc. Natl. Acad. Sci. USA* **117**, 14021-14031 (2020).
- [10] Máthé, M. T., Buka, Á., Jákli, A. & Salamon, P. Ferroelectric nematic liquid crystal thermomotor. *Phys. Rev. E* **105**, L052701 (2020).
- [11] Barboza, R., *et al.* Explosive electrostatic instability of ferroelectric liquid droplets on ferroelectric solid surfaces. *Proc. Natl. Acad. Sci. USA* **119**, e2207858119 (2022).
- [12] Máthé, M. T., Farkas, B., Péter, L., Buka, Á., Jákli, A. & Salamon, P. Electric field-induced interfacial instability in a ferroelectric nematic liquid crystal. <https://arxiv.org/abs/2210.14329>.
- [13] Cmok, L., *et al.*, Running streams of a ferroelectric nematic liquid crystal on a lithium niobate surface, <https://arxiv.org/abs/2209.05140>.
- [14] Yang, J., Zou, Y., Tang, W., Li, J., Huang, M. & Aya, S. Spontaneous electric-polarization topology in confined ferroelectric nematics. *Nat. Commun.* **13**, 7806 (2022).
- [15] Rosseto, M. P. & Selinger, J. V. Theory of the splay nematic phase: single versus double splay. *Phys. Rev. E*, **101**, 052707 (2020).
- [16] Saha, R. *et al.* Multiple ferroelectric nematic phases of a highly polar liquid crystal compound. *Liq. Cryst.* **49**, 1784 (2022).
- [17] Chen, X., Korblova, E., Glaser, M. A., MacLennan, J. E., Walba, D. M. & Clark, N. A. Polar in-plane surface orientation of a ferroelectric nematic liquid crystal: Polar monodomains and twisted state electro-optics. *Proc. Natl. Acad. Sci. USA* **118**, e2104092118 (2021).
- [18] Sebastián, N., Mandle, R. J., Petelin, A., Eremin, A. & Mertelj, A. Electrooptics of mm-scale polar domains in the ferroelectric nematic phase. *Liq. Cryst.* **48**, 2055 (2021).
- [19] Lavrentovich, O. D. Ferroelectric nematic liquid crystal, a century in waiting. *Proc. Natl. Acad. Sci. USA* **117**, 14629 (2020).
- [20] Brown, S., *et al.* Multiple polar and non polar nematic phases. *Chem. Phys. Chem.* **22**, 2506 (2021).
- [21] Nishikawa, H. & Araoka, F. A new class of chiral nematic phase with helical polar order. *Adv. Mater.* 2101305 (2021).
- [22] Rudquist, P. Revealing the polar nature of a ferroelectric nematic by means of circular alignment. *Sci. Rep.* **11**, 24411 (2021).

- [23] Folcia, C. L., Ortega, J., Vidal, R., Sierra, T. & Etxebarria, J. The ferroelectric nematic phase: an optimum liquid crystal candidate for nonlinear optics. *Liq. Cryst.* **49**, 899 (2022).
- [24] Caimi, F., Nava, G., Barboza, R., Clark, N. A., Korblova, E., Walba, D. M., Bellini, T. & Lucchetti, L. Surface alignment of ferroelectric nematic liquid crystals. *Soft Matter* **17**, 8130 (2021).
- [25] Li, J. *et al.*, Development of ferroelectric nematic fluids with giant- ϵ dielectricity and nonlinear optical properties. *Sci. Adv.* **7**, eabf5047 (2021).
- [26] Zhao, X. *et al.* Spontaneous helielectric nematic liquid crystals: Electric analog to helimagnets. *Proc. Natl. Acad. Sci. USA* **118**, e2111101118 (2021).
- [27] Hunter, R. J. & Leyendekkers, J. V. Viscoelectric coefficient for water. *J. Chem. Soc., Faraday Trans. 1* **74**, 450 (1978).
- [28] Andrade, E. N. D. C. & Dodd, C. The effect of an electric field on the viscosity of liquids. *Proc. Roy. Soc. A* **187**, 296 (1946).
- [29] Jin, D., Hwang, Y., Chai, L., Kampf, N. & Klein, J. Direct measurement of the viscoelectric effect in water. *Proc. Natl. Acad. Sci. USA* **119**, e2113690119 (2022).
- [30] Miesowicz, M. The three coefficients of viscosity of anisotropic liquids. *Nature* **158**, 27 (1946).
- [31] Larson, R. G. The structure and rheology of complex fluids. *Oxford University Press, New York* (1999).
- [32] Chmielewski, A. G. Viscosity coefficients of some nematic liquid crystals. *Mol. Cryst. Liq. Cryst.* **132**, 339 (1986).
- [33] Imura, H. & Okano, K. Temperature dependence of the viscosity coefficients of liquid crystals. *Jpn. J. Appl. Phys.* **11**, 1440 (1972).
- [34] Chandrasekhar, S. Liquid Crystals, *Cambridge University Press, Cambridge, England* (1992).
- [35] Ananthaiah, J., Sahoo, R., Rasna, M. V. & Dhara, S. Rheology of nematic liquid crystals with highly polar molecules. *Phys. Rev. E* **89**, 022510 (2014).
- [36] Cidade, M. T., Leal, C. R. & Patricio, P. An electro-rheological study of the nematic liquid crystal 4-n-heptyl-4'-cyanobiphenyl. *Liq. Cryst.* **37**, 1305 (2010).
- [37] Patricio, P., Leal, C. R., Pinto, L. F. V., Boto, A. & Cidade, M. T. Electro-rheology study of a series of liquid crystal cyanobiphenyls: experimental and theoretical treatment. *Liq. Cryst.* **39**, 25 (2012).
- [38] Negita, K. Electrorheological effect in the nematic phase of 4-n-pentyl-4'-cyanobiphenyl. *J. Chem. Phys.* **105**, 7837 (1996).
- [39] Wysocki, J. J., Adams, J. & Haas, W. Electroviscosity of a Cholesteric Liquid-Crystal Mixture. *J. Appl. Phys.* **40**, 3865 (1969).
- [40] Ananthaiah, J., Rajeswari, M., Sastry, V. S. S., Dabrowski, R. & Dhara, S. Effect of electric field on the rheological and dielectric properties of a liquid crystal exhibiting nematic-to-smectic-A phase transition. *Eur. Phys. J. E* **34**, 74 (2011).
- [41] Ananthaiah, J., Sahoo, R., Rasna, M. V. & Dhara, S. Rheology of nematic liquid crystals with highly polar molecules. *Phys. Rev. E* **89**, 022510 (2014).
- [42] Supplementary Information contains details of the synthesis, experimental setup and additional results.
- [43] Dunmur, D. A. Manterfield M. R., Miller, W. H., and Dunleavy, J. K., The dielectric and optical properties of the homologous series of cyano-alkyl-biphenyl liquid crystals. *Mol. Cryst. Liq. Cryst.* **46**, 127 (1978).
- [44] Vaupotič, N., Pociecha, D., Rybak, P., Matraszek, J., Čepič, M., Wolska, J. M. & Gorecka, E. Dielectric response of a ferroelectric nematic liquid crystalline phase in thin cells. <https://arxiv.org/abs/2210.04697>. (2022).
- [45] Clark, N. A., Chen, X., Maclennan, J. E. & Glaser, M. A. Dielectric spectroscopy of ferroelectric nematic liquid crystals: Measuring the capacitance of insulating interfacial layers. <https://arxiv.org/abs/2208.09784>. (2022)
- [46] Mandel, R. J., Sebastián, N., Martínez-Perdiguero, J. & Mertelj, A. On the molecular origins of the ferroelectric splay nematic phase. *Nat. Commun.* **12**, 4962 (2021).
- [47] In our experiment, the measured dielectric constant ϵ in the N_F phase is an effective one for the polydomain texture. We have chosen an optimum frequency (600 Hz) to avoid electrical short-circuit due to the relatively higher ionic electrical conductivity of the bulk sample in the low-frequency range.
- [48] Barthakur, A., Karcz, J., Kula, P. & Dhara, S. Critical splay fluctuations and colossal flexoelectric effect above the nonpolar to polar nematic phase transition. <https://arxiv.org/abs/2211.12471>. (2022).
- [49] Hohenberg, P. C. & Halperin, B. I. Theory of dynamic critical phenomena. *Rev. Mod. Phys.* **49**, 435 (1977).
- [50] We collected the sample from the rheometer after the measurements and checked the phase transition temperatures under polarising optical microscope. We did not observe any noticeable change in the N-I and N- N_F phase transition temperatures after the first scan.
- [51] Ziobro, D., Dziaduszek, J., Filipowicz, M., Dabrowski, R., Czub, J. & Urban, S. Synthesis of fluoro substituted three ring esters and their dielectric properties. *Mol. Cryst. Liq. Cryst.* **502**, 258 (2009).
- [52] Brown, S. *et al.* Multiple polar and non polar nematic phases. *Chem. Phys. Chem.* **22**, 2506 (2021).
- [53] D. G. Hall, in *Boronic Acids*, Wiley-VCH Verlag GmbH & Co. KGaA, Weinheim, Germany, 2011, pp. 1-133.